Data assimilation in the early phase: Kalman filtering RIMPUFF

Astrup, Poul; Turcanu, C.; Puch, R.O.; Palma, C.R.; Mikkelsen, Torben Krogh

Publication date:
2004

Document Version
Publisher's PDF, also known as Version of record

RISØ

Risø-R-1466(EN)

Data assimilation in the early phase: Kalman filtering RIMPUFF

P. Astrup[1], C. Turcanu[2], R.O. Puch[3],
C. Rojas Palma[2], T.Mikkelsen[1]

[1)] Risø National Laboratory, Denmark
[2)] Belgian Nuclear Research Centre (SCK•CEN), Belgium
[3)] University of Warwick, UK

Risø National Laboratory
Roskilde
Denmark
September 2004

Author: P. Astrup, C. Turcanu, R.O. Puch, C. Rojas Palma, T. Mikkelsen
Title: Data assimilation in the early phase: Kalman filtering RIMPUFF
Department: Wind Energy Department

Risø-R-1466(EN)
September 2004

Abstract (max. 2000 char.):

In the framework of the DAONEM project (Data Assimilation for Off-site Nuclear Emergency Management), a data assimilation module, ADUM (Atmospheric Dispersion Updating Module), for the mesoscale atmospheric dispersion program RIMPUFF (Risø Mesoscale Puff model) – part of the early-phase programs of RODOS (Realtime Online DecisiOn Support system for nuclear emergencies) – has been developed. It is built on the Kalman filtering algorithm and it assimilates 10-minute averaged gamma dose rates measured at ground level stations. Since the gamma rates are non-linear functions of the state vector variables, the applied Kalman filter is the so-called Extended Kalman filter.

In more ways the implementation is non standard: 1) the number of state vector variables varies with time, and 2) the state vector variables are prediction updated with 1-minute time steps but only Kalman filtered every 10 minutes, and this based on time averaged measurements.

Given reasonable conditions, i.e. a spatially dense distribution of gamma monitors and a realistic wind field, the developed ADUM module is found to be able to enhance the prediction of the gamma dose field.

Based on some of the Kalman filtering parameters, another module, ToDeMM, has been developed for providing the late-phase DeMM (Deposition Monitoring Module) of RODOS with an ensemble of fields of ground level air concentrations and wet deposited material. This accounts for the uncertainty estimation of this kind of quantities as calculated by RIMPUFF for use by DeMM.

ISSN 0106-2840
ISBN 87-550-3345-8 (Internet)

Also published as
"RODOS(RA5)-TN(04)-01"

Contract no.:
FIKR-CT-2000-00025

Group's own reg. no.:
1100070-1

Sponsorship:
EU-Radiation Protection, FP5

Cover :

Pages: 31
Tables: 0
References: 12

Risø National Laboratory
Information Service Department
P.O.Box 49
DK-4000 Roskilde
Denmark
Telephone +45 46774004
bibl@risoe.dk
Fax +45 46774013
www.risoe.dk

Contents

1 Introduction

In the framework of the Data Assimilation for Off-site Nuclear Emergency Management (DAONEM) project, Rojas-Palma et al. (2001), one of the main objectives is to improve the predictive capability of the RODOS system, Ehrhardt and Weiss (2000), by combining model predictions with observations. Through this process, observations will be used to update model results for as long as they are needed for decision support purposes, Kelly et al. (1996). It is also expected that DAONEM would contribute to the transfer of uncertainties from one RODOS module into to subsequent one; thus making uncertainty a vital piece of information for decision-making.

During the early phase of an atmospheric release of radioactivity, spanning from the pre-release and extending not beyond 24 hours from its onset, the decision making process will concentrate on sheltering, distribution of stable iodine, and, if need be, evacuation. All these countermeasures will be strongly supported by model predictions, which are prone to errors and uncertainties. After some time, monitoring teams and radiological networks will start populating a database; however, these data may be sparse in both time and space and therefore model predictions will still be needed.

The present report describes the Atmospheric Dispersion Updating Module (ADUM), i.e. the data assimilation module developed for the atmospheric dispersion model RIMPUFF, Risø Mesoscale Puff Model, Mikkelsen et al. (1984), Thykier-Nielsen et al. (1998), one of the dispersion models in the Local Scale Model Chain of RODOS. The prescribed data assimilation method in DAONEM is the so-called Kalman filtering, Kalman (1960), which updates selected state variables of the prediction on the basis of differences between predicted and measured quantities and on uncertainty estimates for both prediction and measurements. Because of the nonlinearity between the selected state variables: puff position and inventory, and the available measurement quantities: gamma dose rates, the so-called Extended Kalman Filter has been applied.

More than just being post-processed by other early-phase RODOS modules, the RIMPUFF/ADUM results are also needed by the later phase Deposition Monitoring Module (DeMM), Gering et al. (2000). In DeMM, Kalman filtering is also being applied, for which reason uncertainty estimates have to follow the fields passed to it. DeMM does this estimation itself based on an ensemble of probable fields, and for the calculation of this ensemble of fields, the ToDeMM module has been created, a module also described in the present report.

2 Acknowledgement

The reported work has been supported by the European Commission under the project “Data Assimilation for Off-site Nuclear Emergency Management” (DAONEM), contract N° FIKR-CT-2000-00025.

3 RIMPUFF

The early-phase atmospheric dispersion model used in this project is the Risø Mesoscale Puff model, RIMPUFF, Mikkelsen et al. (1984), Thykier-Nielsen et al. (1998), which is driven by a meteorological preprocessor. RIMPUFF models the plume of released material as a number of individual puffs, every 10 minutes releasing a puff that holds 10 minutes of released material. A puff can be visualized as a kind of spherical or ellipsoidal cloud, a body of air and suspended

released material, having a certain size. For the sake of calculation, the suspended material is given a 3D-Gaussian concentration distribution. This is an approximation to the real fluctuating distribution in a plume, and at its tails it is not describing reality very well. For this reason RIMPUFF cuts it off at a user specified distance from the puff centre, the point of maximum concentration. The recommended cut-off distance is 3.7 standard deviations, where the concentration equals 0.001 times the centre concentration, and with this value RIMPUFF accounts for 97% of the specified release, far within any real release uncertainty.

Each puff is advected with the local wind speed at its centre, it grows in size due to the local turbulence - i.e. the concentration distribution flattens - its centre is raised as the puff strikes the ground in order to model the rise of the plume centre of mass, and its inventory holds up to 15 different nuclides, the amount of which change due to radioactive decay and due to deposition to ground, the latter due to both dry processes and to rain. All meteorological parameters needed by the model are obtained from the meteorological pre-processor of RODOS.

RIMPUFF delivers fields of time integrated ground concentrations, time integrated gamma dose rates (i.e. gamma doses) from the puffs, time integrated deposition rates (i.e. deposited amount) split on dry and wet deposition, and instantaneous gamma dose rates from deposited material, all for each of the up to 15 nuclides. Iodine is further treated as a mix of differently depositing elementary, organic, and aerosol bound iodine. And more than just the fields, RIMPUFF also calculates the same parameters for specific points, detector points, specified within the computation area.

4 Kalman filtering

Kalman filtering, Kalman (1960), is a statistically based method for improving model predictions by real time assimilation of measurements. It works by updating the state vector, i.e. a set of important state variables in the model being filtered, by applying a correction based on the difference between measured and model calculated data and on specified uncertainties associated with the state vector update and with the measurements. The methodology and the used nomenclature are described in appendix A, and in more detail in Puch and Astrup (2002).

For normal Kalman filtering of a well posed system, the state vector is a constant set of parameters, the Kalman update takes place at every time step based on instantaneous measurements, and the P-matrix, the error covariance matrix, settles after a number of time steps and becomes more or less constant in time, holding values that do not depend on its initial setting.

For the Kalman filtering of RIMPUFF the state vector has been selected to hold the centre position (x,y,z) and the total radioactive content q of each puff within the given computation domain, whereas the data used for the Kalman filtering are the calculated and measured gamma radiation dose rates at the specified ground based detector points.

Already here two things make this use of Kalman filtering non standard: 1) The state vector variables are not a fixed set but change whenever a new puff is released, a puff leaves the calculational area, or a puff splits into more puffs, and 2) measured gamma dose rates shall only be available as 10-minute average values, i.e. the Kalman filter has to update "instantaneous" puff positions and contents based on calculated and measured 10-minute average values.

Using 10-minute average gamma dose rates is not necessarily a draw back. In fact the calculated instantaneous gamma dose rates to the detector points on ground shall be artificially fluctuating due to the split of the plume into puffs, which at least close to the release point are so small that they do not really overlap if there is just a bit of wind. The 10-minute average values can be

considered more reliably calculated quantities. But the determination of the needed derivatives of the 10-minute average dose rates with respect to the final puff positions is not unique.

A third untypical element comes in, if the detector points are sparse and puffs may travel several time steps before getting sufficiently close to the next detector point to add to the dose rate there. In this case different parts of the state vector may get Kalman updated at different times and not necessarily often.

4.1 Error covariance matrix initialization

The behaviour of the Kalman filtering is very much dependent upon the so-called *P*-matrix, the error covariance matrix, which is updated during the Kalman procedure, but needs to be initialized. For normal well-behaved Kalman filtering, the *P*-matrix stabilizes after some update sequences, and the initial value is not critical, but, as mentioned above, the actual use of Kalman filtering is not standard, and the initial *P*-matrix is very influential.

As the Kalman state vector contains the center position *(x,y,z)* and the inventory q of each puff, and the P-matrix holds the error covariances of all state vector variables, the *P*-matrix expands, whenever a new puff is released. All new parameters, i.e. all parameters refering to the new puff, need to be initialized. The covariance elements for the new puff itself, the submatrix P_{init}, is set as

$$P_{init} = \begin{pmatrix} S_{xy}^2 & 0 & 0 & 0 \\ 0 & S_{xy}^2 & 0 & 0 \\ 0 & 0 & S_z^2 & 0 \\ 0 & 0 & 0 & (a \cdot q)^2 \end{pmatrix}$$

where S_{xy}, S_z, and a are user specified numbers, while q is the also user specified total puff activity for the new puff.

The S_{xy} and S_z values represent the standard deviation of the initial puff position, i.e. the uncertainty of the release point position, horizontally and vertically.

The coefficient $a=S_q/q$ specifies the ratio of the puff inventory standard deviation S_q to the specified puff inventory q, i.e. it is the relative uncertainty in the estimation/specification of the release rate.

The covariances between new puff and old puff state vector variables also form submatrices in the *P*-matrix, which need initialization. The off-diagonal terms are again set to 0.0, while the diagonal terms are set as half the sum of the corresponding *P*-matrix diagonal terms multiplied with a factor going smoothly from 1 to 0 for the puff-to-puff distance going from 0 to twice the Lagrangian length scale of the local atmospheric turbulence.

4.2 Prediction update covariances

The Kalman filter needs an error covariance estimate for the prediction update of the state vector. A method for estimating these error covariances for the state vector variables of a single puff and of different puffs is presented in appendix B. With a single adjustment the method presented there is the one being used.

The adjustment is due to the fact, that the approach of appendix B is based on wind speed and direction uncertainties due only to turbulence, any meteorological bias thus being neglected. Bias as such cannot be dealt with, but the uncertainties can be increased due to the expectation of other uncertainty sources than just turbulence. Presently a hardwired minimum wind direction

uncertainty (standard deviation) is applied: $\sigma_{\varphi}. \geq 15°$, while for a neutrally stable atmosphere the appendix B formulas give $\sigma_{\varphi} \approx 6°$.

4.3 Measurement covariances

Kalman filtering also needs an estimation of the measurement uncertainties, or more precisely, it needs a covariance matrix for the measurements. For the present implementation zero covariance is assumed between different measurements thus reducing the problem to the vector of the matrix diagonal, i.e. the measurement variances. Radiation monitoring devices are different and so are their uncertainties/variances. For the time being the RODOS system is not set up to provide uncertainty information for which reason it is necessary to specified it via file input. This has been made simple and it is based on an instrument at Risø National Laboratory, Denmark. The measurement standard deviation is set as the maximum of a fraction *f* of the measured gamma dose rate *y* and a minimum uncertainty value *m*:

$$\sigma = \max(f * y, m)$$

The applied variances equal σ^2.

f and *m* are user specified, and only a single set can be given. This is then used for all specified detectors.

4.4 Averaging details

The Kalman filtering on measured 10-minute average gamma dose rates requires that the predicted gamme dose rates are also 10-minute average values. When a puff passes a detector point the calculated dose rate there can vary rather quickly, and a single instantaneous dose rate per minute, as calculated by RIMPUFF, may be inappropriate for the averaging. To obtain better gamma dose rate averages, the puff positions and inventories are therefore interpolated into 6 seconds steps, i.e. 10 steps per puff advection step, and the gamma dose rates so averaged over 100 instantaneous values in stead of 10. This is performed in a complex of routines not being part of RIMPUFF although with calls to the RIMPUFF gamma dose rate routines, and called from within the RIMPUFF one-minute timestep advection loop.

The matrix elements holding derivatives of the gamma dose rates at the detector points with respect to puff positions and inventories are calculated in parallel to the gamma dose rates and also averaged over 100 six-second values.

5 Test cases

Test cases are necessary for the development of simulation tools. In the present development of Kalman filtering for the RIMPUFF dispersion model, the "measurement data" have mostly had to be produced by the code itself and then used for the filtering in tests with slightly changed wind or release conditions.

5.1 Proof of concept

The first test case was a kind of proof of concept . It was not carried out with RIMPUFF but with a small purpose built program using a straightforward implementation of an extended Kalman filter based on instantaneous gamma dose rates and updating after every 60-second time step. It involved a single puff only, and the state vector only comprised the puff centre coordinates, not the inventory.

A dry run (no Kalman filtering) was performed with a specified pure westerly wind, i.e. wind direction 270°. At three detector points 1000 m right east of the release point and with 20 m north/south separation the received instantaneous gamma dose rates were calculated and stored for use as "measurements" in following calculations.

The next calculation was still without Kalman filtering but with a wind direction 10° south of west, i.e. 260°. No calculated gamma dose rates were stored, just the track of the puff.

The third calculation then was the real test. The wind direction was again the 260° while the Kalman filter used the "measurements" created in the 270° wind direction calculation. The result can be seen in Figure 1. When the puff gets close enough to the detector points the *H*-matrix, which holds the derivatives of the detector point gamma rates with respect to the puff centre coordinates, gets different from zero, and the Kalman update makes the puff deviate from its wind given course and more or less follow the path of the puff that has created the "measurements". Simultaneously the error covariances decrease. When the puff again gets further from the detector points, then $H = 0$, the error covariances increase, and the puff again follows the wind.

5.2 Cases with internally generated "measurements"

All other reported test cases have been performed with the final RODOS integrated RIMPUFF/Kalman system, and all but one with "measurements" generated by the code itself in an initial no-Kalman run. For these cases the release point has been Risø, Denmark, and there have been 8 detector points surrounding Risø at a distance of 2 km and 15 other detector points in a 5*3 array, the 5 midpoints being 10, 20, 30, 40 and 50 km right east of Risø, the other points 5 km right north and south of the midpoints, all in all 23 detector points. The 15 points of the array are shown in figure 2 but the 8 points surrounding Risø are not, as they should just clutter the figure. The resolution of the computation grid is 2 km.

The "measurements" at the 23 detector points have been created in a "base" run with 2 hours release of pure ^{137}Cs, release rate 10^{18} Bq/h, release height 60 m above ground, no heat in the release. The meteorological situation was strict westerly wind, 7 m/s at 60 m above ground at Risø, neutral stability, no rain. Figure 2 shows the gamma dose field (time integrated gamma dose rates) of this calculation on the background of the land cover map.

5.2.1 Cases with change in release rate

Some cases have been run with change just in the release rate, and with different uncertainties "*a*" specified for this rate. Figure 3 shows results for half and double release rate and Kalman filtering just based on the 8 detectors surrounding Risø, while in figure 4 the rates have been 10 times and 1/10th the base rate and Kalman filtering have been based on all 23 detector points. In all cases the results shown are for the detector point 50 km right east of Risø. Figures 5 and 6 show the fields of gamma doses for these cases. It is clear that the specification of the release uncertainty is of importance and that in these cases the higher tried values prove the better. It is also clear that the 1/10th release case requires a larger release uncertainty that the 10-fold release case.

5.2.2 Cases with change in wind direction

With the release rate as in the base run but the wind shifted 5° south, runs with the Kalman filtering based on 8, 11 or all 23 detector points have been performed. The 8 points are those surrounding Risø, the 11 the same plus the easternmost column of the array points. Again calculations have been made for different assumed release rate uncertainties. Figure 7 shows the resulting gamma dose rates for the 11 and 23 points Kalman filtering at the point 50 km straight east of Risø. In this case with "correct" release rate it is not surprising, that the low value of the release uncertainty proves best, a result further highlighted by figures 8 and 9, where the gamma dose fields calculated for the two Kalman filtering configurations are shown.

For the a = 0.1 calculations, figure 10 shows the influence of the number of detector points used for the Kalman filtering, or rather the influence of the density of these points. It is clear that the higher density, the better. The same can be seen from figures 8b and 9b.

5.2.3 Cases with change in both release rate and wind direction

With the wind 5° south of west, i.e. 5° off the base wind, and with the release rate 10 and 1/10 the base release rate a number of cases have been run with different release rate uncertainties. Figures 11 and 12 show the results. As for the cases with only release rate changes, the results get better with the higher release rate uncertainties.

Also for wind 10° off and 1/10th release rate, the higher release rate uncertainty, a=5, proves best, figure 13. Not shown but also tested here is a=10. This made however no enhancement as compared to a=5.

5.3 Cases with externally generated "measurements"

In order to test the system against data not generated by itself, we got help from Rijksinstitut voor Volksgezondheid en Milieu (RIVM) in the Netherlands. Dr. Yvo Kok, Yvo Kok (2003), provided us with gamma dose rate "measurements" for the real operational Dutch detector points, as calculated with the dispersion code of RIVM, simulating a 4-hour release from the Borssele nuclear power station, starting 25th September 2003, 0600 UTC. The driving meteorology was field data of the HIRLAM numerical weather prediction model of Koninklijk Nederlands Meteorologisch Instituut (KNMI). The HIRLAM model, Sass (1994), is being developed by a cooperation of European meteorological institutes including the Danish Meteorological Institute and the KNMI. An extract of the used meteorological field data, i.e. data representative for a point near the point of release, plus source terms were also provided. This is believed to be the most realistic simulation we can make of a real case where a plant fails, the released material is dispersed by the atmosphere, and the best meteorological data available are those measured close to the failing plant.

After a first test we added 12 virtual detector points surrounding the Borssele plant at a distance of 1 km.

Figure 14 shows - on the background of the land use map - the field of gamma doses as calculated and interpolated from the provided gamma dose rates for the irradiated detector points within the computation area. The surrounding but not irradiated points are not used for this plot. The points numbered on the plot are the real detector points, the three irradiated virtual points are not shown. Figure 15 presents the equivalent RIMPUFF calculation based on the one point meteorology and with no Kalman filtering applied. The two plumes cover almost the same area, but it is quite clear, that the RIMPUFF results are rather different from those of RIVM, although only the values at the detector points and not the fields as such should be compared.

With the RIVM calculated detector point values used as measurements, Kalman filtering of the RIMPUFF calculation has been carried out in five different ways, based 1) on the values of the real detector points only, 2) on the values of the 12 virtual detector points only, and 3) on the values of both sets of detector points, all for release rate uncertainty a=0.1. Further, for release uncertainty a=1.0 and Kalman filtering on all detector points, with 4) specified release rate and 5) double of specified release rate. The resulting gamma dose rates for 8 of the detector points are shown in figure 16 together with results for no Kalman filtering and with the RIVM data. Comparing RIVM and RIMPUFF without Kalman filtering the difference in maximum rates but especially the difference in irradiation times at the different points is striking, RIVM giving far the longest times. The only exception to this is at point 140, which is very close to the release point. The "RIMPUFF without Kalman" curve cannot be seen in this "point 140" plot as it collapses with the "Kalman on

real points" curve. It is clear, that the two models, RIVM and RIMPUFF, cannot both be close to being correct, was this a real case. The RIVM model exposes most points for a much longer time than does RIMPUFF and with a comparable dose rate, so it produces a rather much higher dose at these points.

The effect of the different Kalman filterings is better seen from dose plots than from dose rate plots, and figure 17 shows the figure 16 equivalent doses. It can be seen that with a release rate as specified by RIVM and the release rate uncertainty a=0.1, the Kalman filtering on only the real points leads to an enhanced prediction for only three of the 8 points plotted, and only marginally for two of these, while inclusion of the 12 virtual detector points around the release point makes the Kalman filter enhance the results at all 8 points except at point 140, the point close to the release point, although again only marginally for most of the points. Setting the release rate uncertainty to 1.0 instead of 0.1 increases the gamma doses at all points except point 143, the results at most points getting better. Combining a=1.0 with double release doesn't help here.

For some combinations of parameters, this Borssele release case also causes the Kalman filter to move a single puff far away from a reasonable position, figure 18. The tendency for such behaviour has, however, been greatly reduced by limiting the detector points actually used for Kalman filtering of a given puff to only those having gamma rate derivatives with respect to the puff inventory exceeding 10% of the maximum found for all the points, with other words by excluding detector points which do not really see the puff.

All in all the Kalman filtering does generally enhance the calculated gamma doses in this most realistic case, especially for a=1. And it is the impression that it is the huge difference between the RIVM and the basic RIMPUFF predictions plus the sparsity of the detector points that prevent a better result.

6 ToDeMM

The results of the RIMPUFF/Kalman modules, are used as input to other early-phase RODOS modules, e.g. the dose module and the arrival time module, and to later phase modules of RODOS, especially to the Deposition Monitoring Module (DeMM), Gering et al. (2000), which requires fields of time integrated air concentrations at ground level and the amounts of wet deposited material for each of the actual nuclides. And in order to apply Kalman filtering in DeMM, this module also needs an estimate of the uncertainty of the provided fields.

DeMM itself makes this estimate, and what is presented here is the so far last method in a series of more or less similar methods for providing data for this estimation. It still awaits testing with DeMM.

6.1 Ensemble of results

DeMM applies a so-called Ensemble Kalman filter, so the information to base the uncertainty estimate on is provided as an ensemble of 100 sets of normal RODOS fields of time integrated concentrations and wet depositions, each set being a kind of possible RIMPUFF outcome, the actual RIMPUFF calculated results forming one of the sets.

Running RIMPUFF one hundred times with perturbed wind and release rates is not feasible. Instead we take advantage of the error covariance matrix, the P-matrix used in the Kalman module and updated in the RIMPUFF prediction steps as well as in the Kalman filtering steps.

6.2 Generation of ensemble results

At each time step, an ensemble of 100 state vectors are created by perturbing the actual Kalman state vector, i.e. position and content *(x,y,z,q)* of all puffs, into 99 other possible state vectors. The perturbations are based on the actual error covariance matrix plus 99*4 numbers, $Z_{1,1}$,$Z_{1,2}$,...,$Z_{99,4}$, stochastically drawn from a unit variance Gaussian distribution. To make perturbed ensemble member N, 1≤N≤99, simulate a possible RIMPUFF answer, the same four Gaussian numbers, ($Z_{N,1}$, $Z_{N,2}$, $Z_{N,3}$, $Z_{N,4}$), are used for the perturbation of all the state vector variable parts *(x,y,z,q)*, i.e. for all the puffs. At each time step we thus calculate:

$$PC = Cholesky(P)$$

$$X_1 = X + PC \cdot (Z_{1,1}, Z_{1,2}, Z_{1,3}, Z_{1,4}, Z_{1,1}, Z_{1,2}, Z_{1,3}, Z_{1,4}, ..., Z_{1,1}, Z_{1,2}, Z_{1,3}, Z_{1,4})$$

$$X_2 = X + PC \cdot (Z_{2,1}, Z_{2,2}, Z_{2,3}, Z_{2,4}, Z_{2,1}, Z_{2,2}, Z_{2,3}, Z_{2,4}, ..., Z_{2,1}, Z_{2,2}, Z_{2,3}, Z_{2,4})$$

.....

$$X_{99} = X + PC \cdot (Z_{99,1}, Z_{99,2}, Z_{99,3}, Z_{99,4}, Z_{99,1}, Z_{99,2}, Z_{99,3}, Z_{99,4}, ..., Z_{99,1}, Z_{99,2}, Z_{99,3}, Z_{99,4})$$

where X is the actual state vector and PC is the Cholesky decomposition of the actual error covariance matrix P. In this way all puffs in an ensemble, are displaced in coherent directions, and the inventory is perturbed in a way that may simulate a coherent perturbation in wet deposition. For each ensemble member the corresponding fields of ground level time integrated concentration and wet deposition are calculated using the formulas and models from RIMPUFF. Figure 19 shows for a case of southerly wind the mean of the concentration fields of the 100 ensemble members compared to the field of unperturbed RIMPUFF alone.

To save disk space, data of the final fields are only saved for grid points where the data are different from 0, typically reducing the needed space from around 30 to around 2 Mbyte.

7 Conclusion

A Kalman filtering module has been created for the Risø Mesoscale Puff dispersion model RIMPUFF built into RODOS. Based on predicted and measured 10-minute averaged gamma dose rates, it updates the state of the modelled puffs, i.e. their position and their content of radioactivity. And a separate but anyway connected module has been created to give uncertainty information for a following RODOS late phase deposition monitoring module, which implements an Ensemble Kalman filter.

Kalman filtering is intended for updating predictions with the help of measurements, keeping this difference small. The test cases indicate that, given reasonable circumstances, the developed Kalman filter enhances the predictive capability of the RIMPUFF model so that the gamma dose predictions get closer to those measured than what is found without applying Kalman filtering. "Reasonable circumstances" here means a reasonably tight net of detector points, a reasonably well specified wind field, and a reasonable accurate release rate.

The test cases also indicate that RIMPUFF as such, and the Kalman filtering of it, should benefit from a model that could limit the source specification error. Such a model might be based on a large amount of spatially distributed on site and near off site spectral gamma measurements, on site meteorology, and known plant status. It could be one that does not anticipate a certain form of the cloud but makes a kind of variational calculation on the 3D concentration distribution around the plant, or may be just a simpler iteratively optimized Gaussian plume model.

Another achivement with potential of enhancing the outcome of the presented model is data assimilation of the Numerical Weather Prediction model forecasts used as input to the RODOS meteorological pre-processor which delivers the needed meteorological fields for the dispersion calculation. Such work is under way, Kovalets et al. (2004).

8 Figures

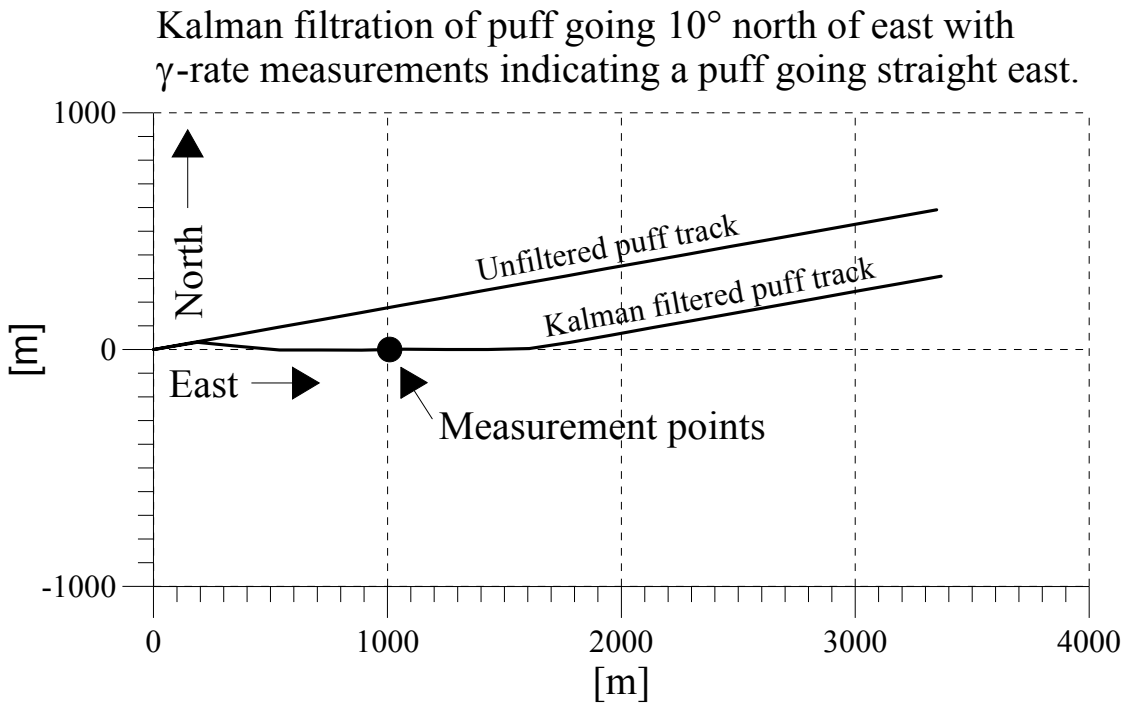

Figure 1: Track of puffs following a wind going 10 ° north of east, one unfiltered and one Kalman filtered with measurements indicating a puff going straight east.

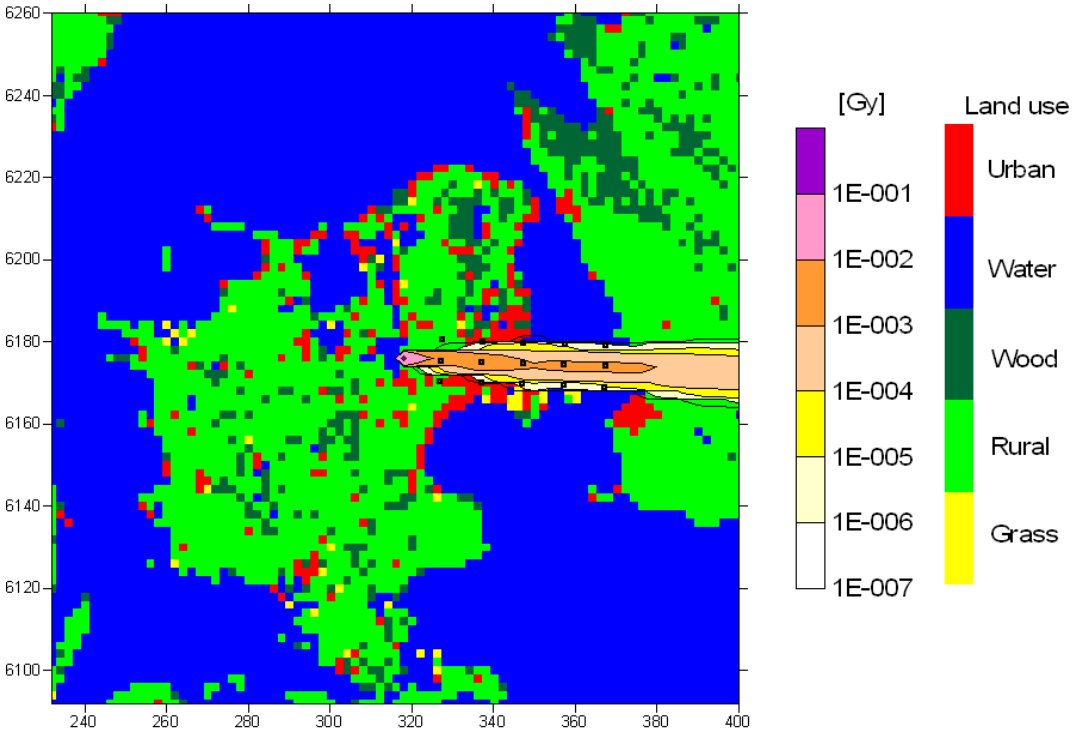

Figure 2: Gamma dose field from puffs in measurement generating run. The 15 detector points 10 to 50 km east of the release point are seen as black squares, the 8 points surrounding the release point are not marked. The background picture is the land use map.

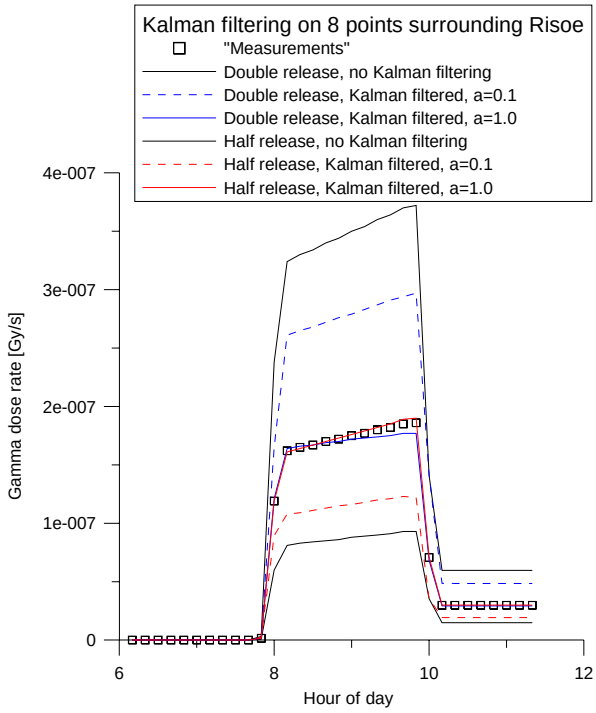

Figure 3: Gamma dose rates 50 km from the release point, right below the plume. Kalman filtering applied in runs with the release doubled and halved relative to that having generated the "measurements", and with different release rate uncertainties "a".

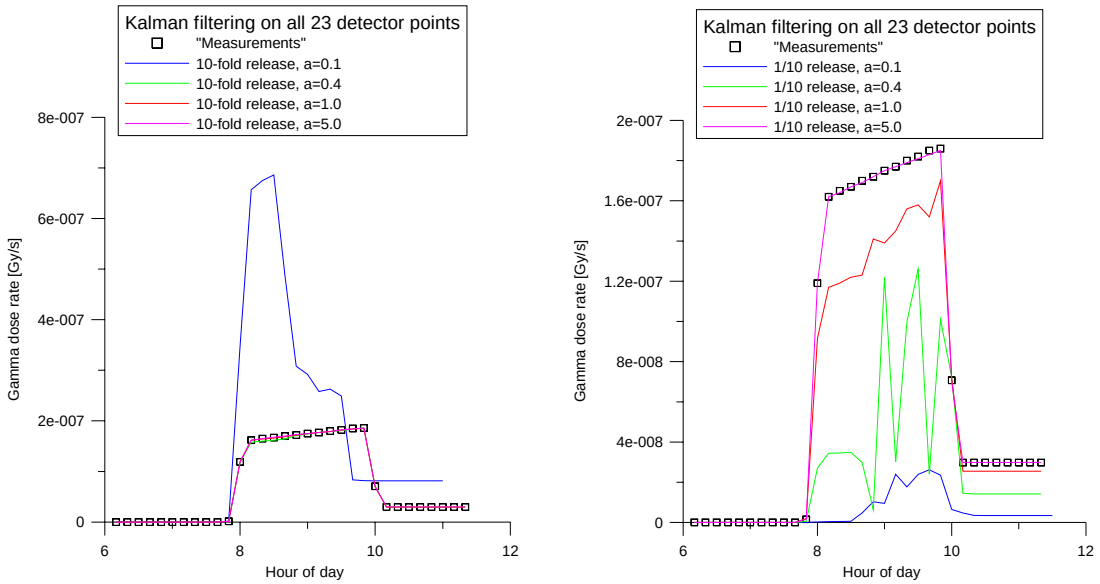

Figure 4: Gamma dose rates 50 km from the release point, right below the plume. Kalman filtering applied in runs with the 10 fold and 1/10th release of that having generated the "measurements", and with different release rate uncertainties "a".

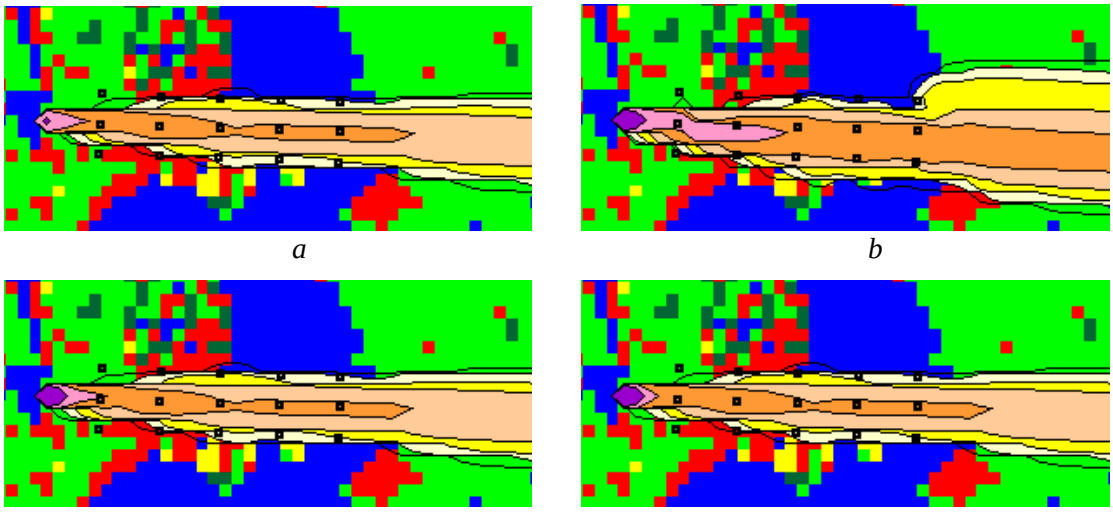

Figure 5: Kalman filtering applied in runs with 10 fold the release having generated the "measurements", and with different release uncertainties "a". a) Measurement run. Relative release rate uncertainties: b) a=0.1, c) a=0.4, d) a=1.0.

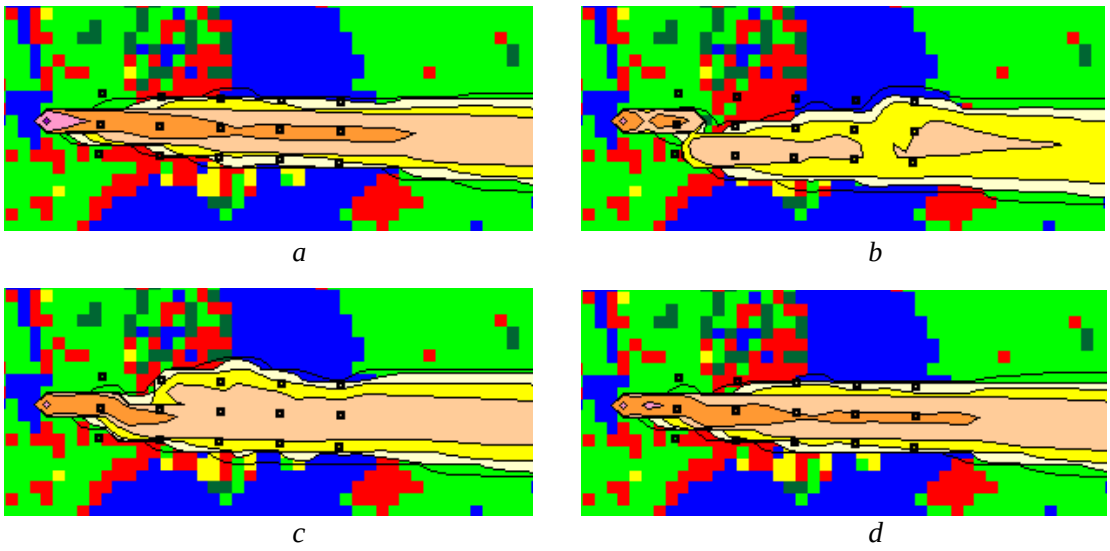

Figure 6: Kalman filtering applied in runs with 1/10th the release having generated the "measurements", and with different release uncertainties "a". a) Measurement run. Relative release rate uncertainties: b) a=0.1, c) a=0.4, d) a=1.0.

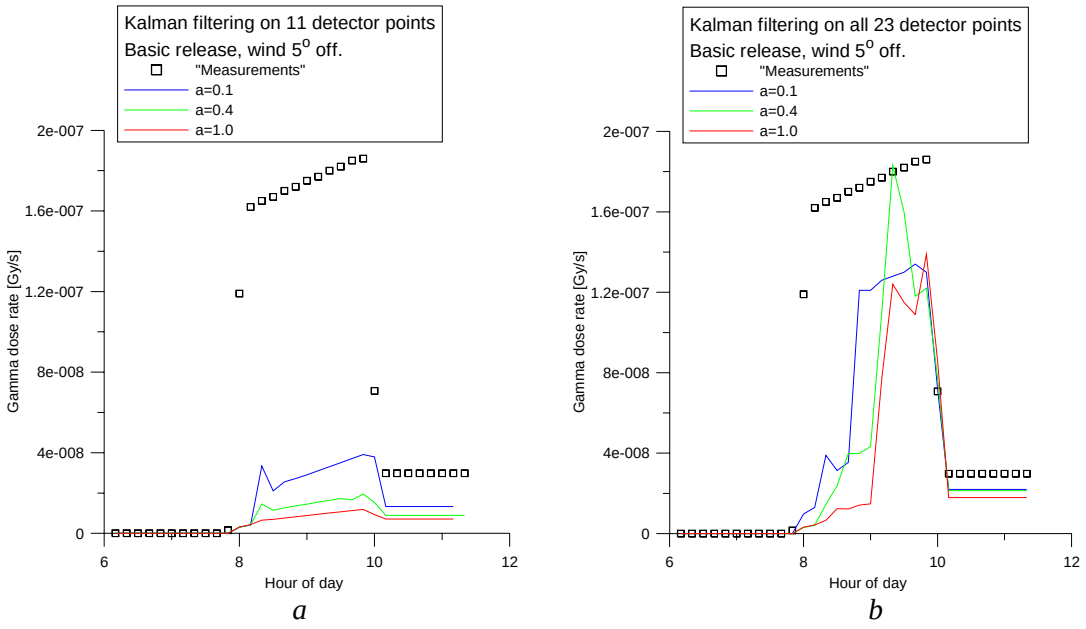

Figure 7: Gamma dose rates 50 km right east of the release point with wind 5° south of west. Kalman filtering on the 8 detector points surrounding the release point plus: a) the 3 eastern most detector points and, b) all 15 array detector points. All for different release rate uncertainties "a".

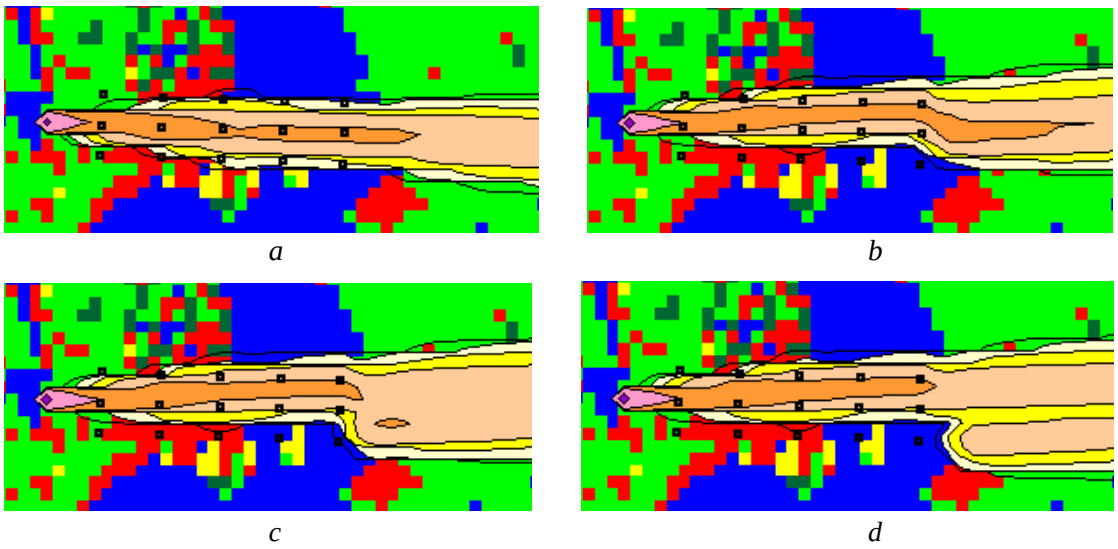

Figure 8: Gamma dose rates fields with wind 5° south of west. Kalman filtering on the 8 detector points surrounding the release point plus the 3 eastern most detector points. a) Measurement run. Relative release uncertainties: b) a=0.1, c) a=0.4, d) a=1.0.

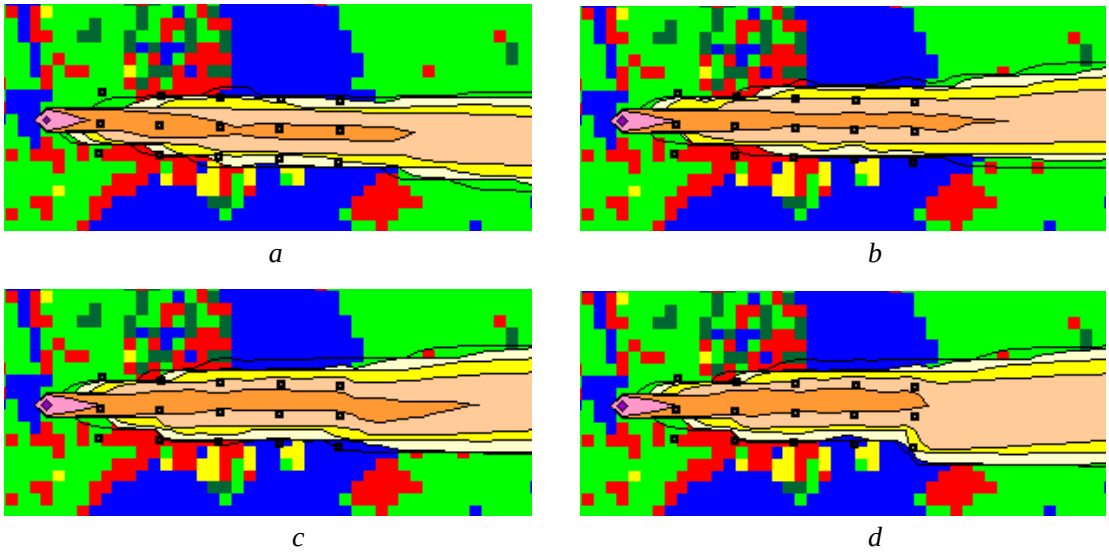

Figure 9: Gamma dose rates fields with wind 5° south of west. Kalman filtering on the 8 detector points surrounding the release point plus all 15 array detector points. a) Measurement run. Relative release uncertainties: b) a=0.1, c) a=0.4, d) a=1.0.

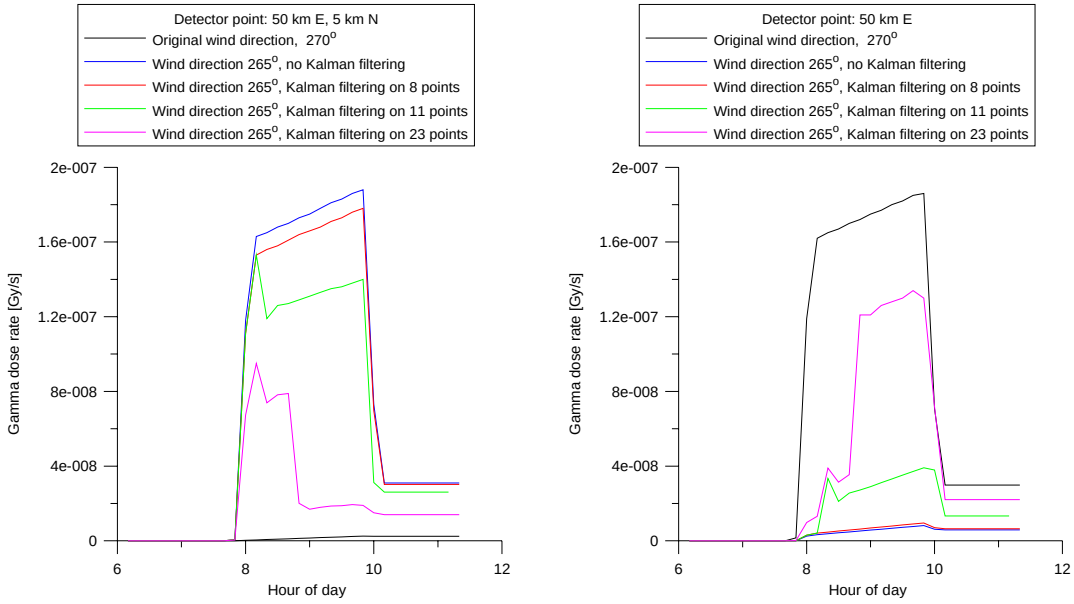

Figure 10: Gamma dose rates at northernmost and central detector point 50 km east of release point. Wind 5° south of west. Kalman filtering on different amounts of detector points. Relative release unvertainty a=0.1.

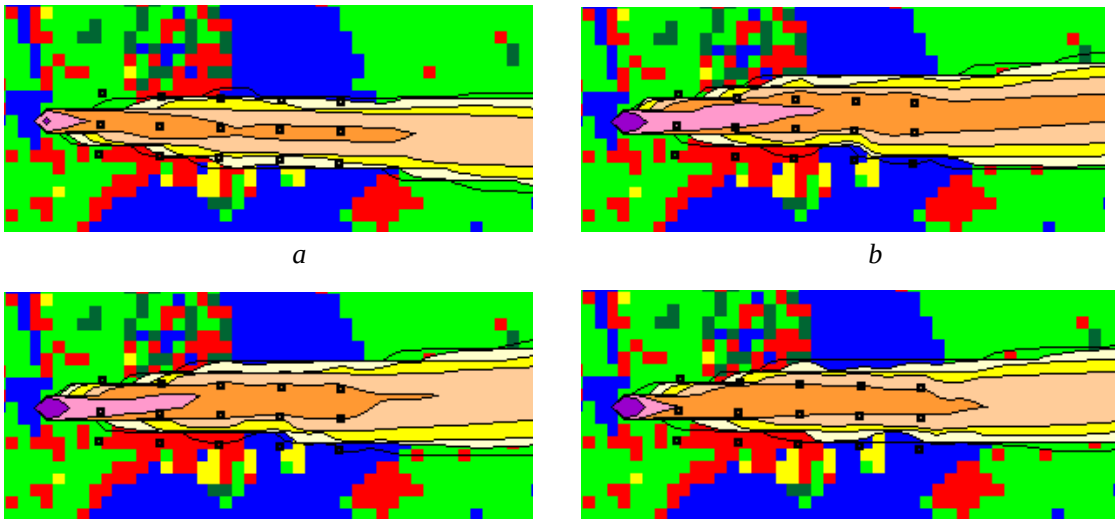

Figure 11: Gamma dose rates fields with wind 5° south of west and 10 fold release rate. Kalman filtering on all 23 detector points. a) Measurement run. Relative release uncertainties: b) a=0.4, c) a=1.0, d) a=5.0.

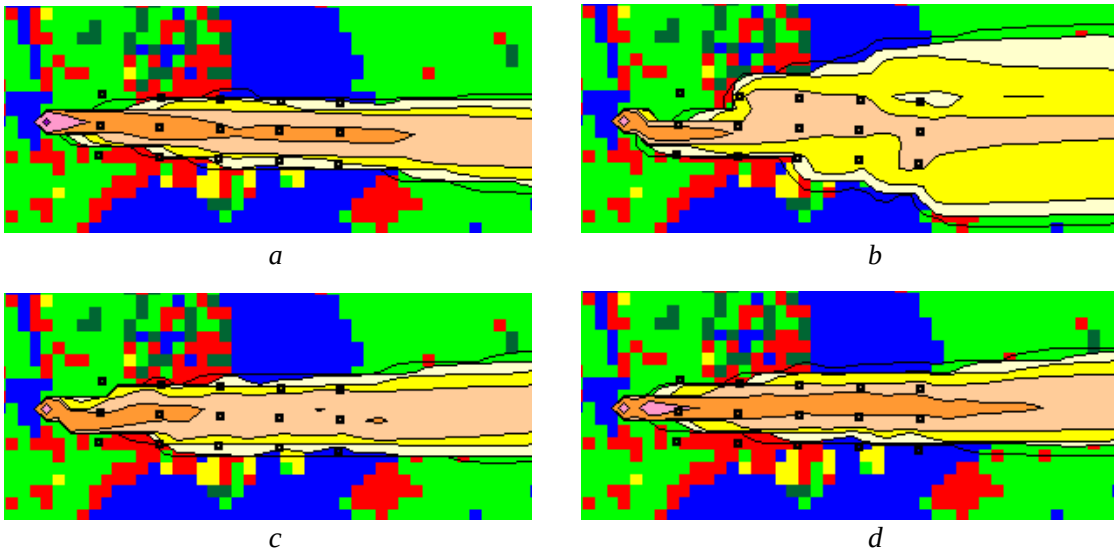

Figure 12: Gamma dose rates fields with wind 5° south of west and 1/10th release rate. Kalman filtering on all 23 detector points. a) Measurement run. Relative release uncertainties: b) a=0.4, c) a=1.0, d) a=5.0.

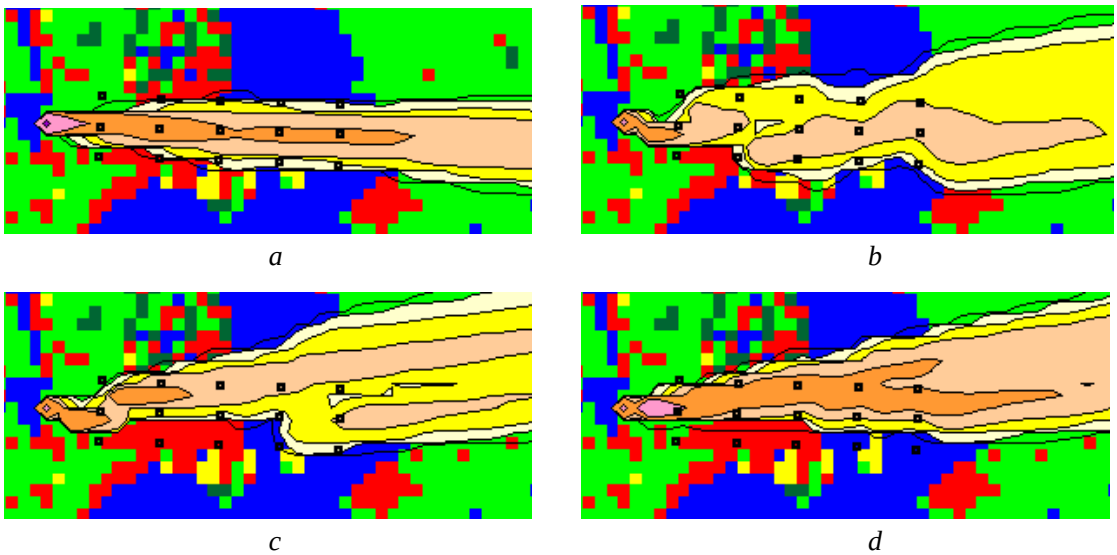

Figure 13: Gamma dose rate fields with wind 10° south of west and 1/10th release rate. Kalman filtering on all 23 detector points. a) Measurement run. Relative release uncertainties: b) a=0.4, c) a=1.0, d) a=5.0.

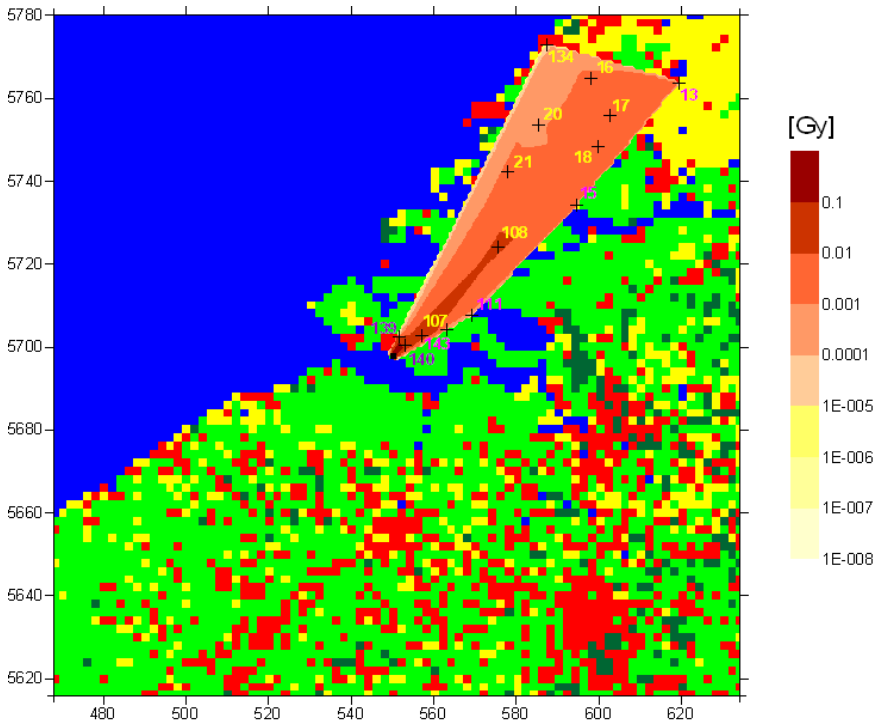

Figure 14: Plot based on time integrated gamma dose rates as calculated by RIVM. The numbered detector points (crosses) are the real Dutch detector points having received gamma doses in the RIVM calculation.

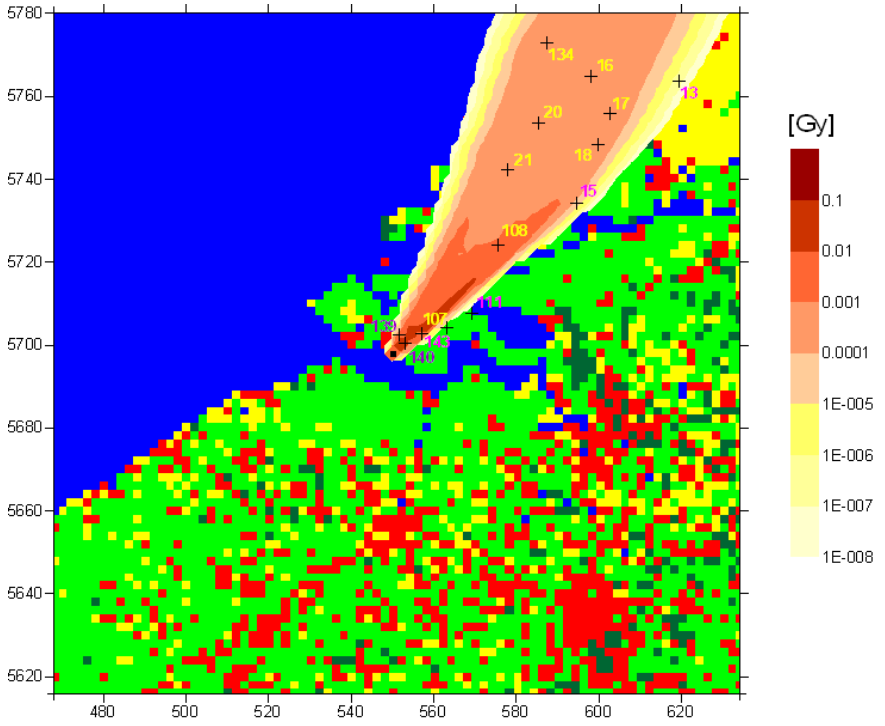

Figure 15: Time integrated dose rates as calculated by RIMPUFF based on one point meteorological data from RIVM (KNMI). No Kalman filtering.

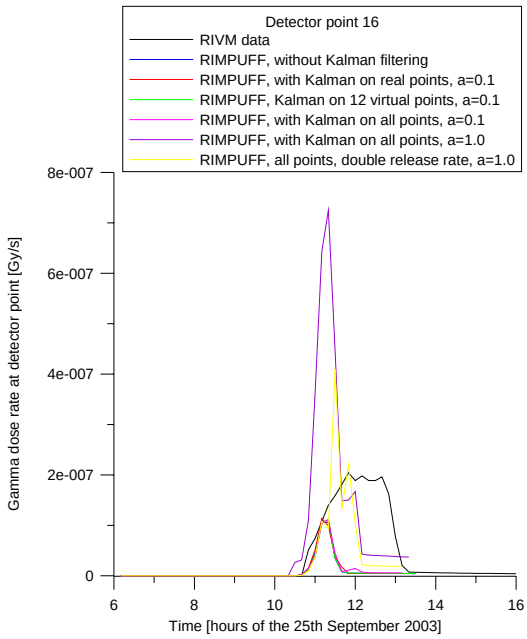
Detector point 16
RIVM data
RIMPUFF, without Kalman filtering
RIMPUFF, with Kalman on real points, a=0.1
RIMPUFF, Kalman on 12 virtual points, a=0.1
RIMPUFF, with Kalman on all points, a=0.1
RIMPUFF, with Kalman on all points, a=1.0
RIMPUFF, all points, double release rate, a=1.0
Gamma dose rate at detector point [Gy/s]
8e-007
6e-007
4e-007
2e-007
0
6
8
10
12
14
16
Time [hours of the 25th September 2003]

a

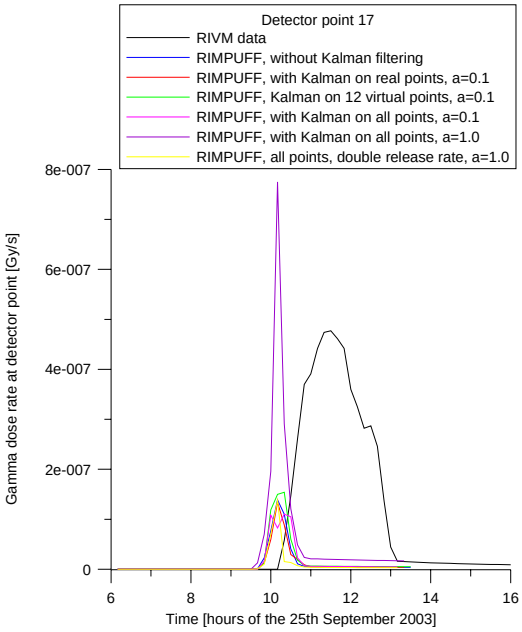
Detector point 17
RIVM data
RIMPUFF, without Kalman filtering
RIMPUFF, with Kalman on real points, a=0.1
RIMPUFF, Kalman on 12 virtual points, a=0.1
RIMPUFF, with Kalman on all points, a=0.1
RIMPUFF, with Kalman on all points, a=1.0
RIMPUFF, all points, double release rate, a=1.0
Gamma dose rate at detector point [Gy/s]
8e-007
6e-007
4e-007
2e-007
0
6
8
10
12
14
16
Time [hours of the 25th September 2003]

b

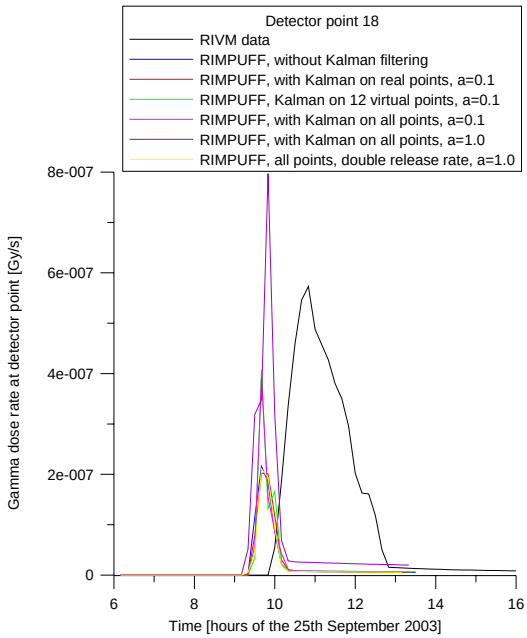
Detector point 18
RIVM data
RIMPUFF, without Kalman filtering
RIMPUFF, with Kalman on real points, a=0.1
RIMPUFF, Kalman on 12 virtual points, a=0.1
RIMPUFF, with Kalman on all points, a=0.1
RIMPUFF, with Kalman on all points, a=1.0
RIMPUFF, all points, double release rate, a=1.0
Gamma dose rate at detector point [Gy/s]
8e-007
6e-007
4e-007
2e-007
0
6
8
10
12
14
16
Time [hours of the 25th September 2003]

c

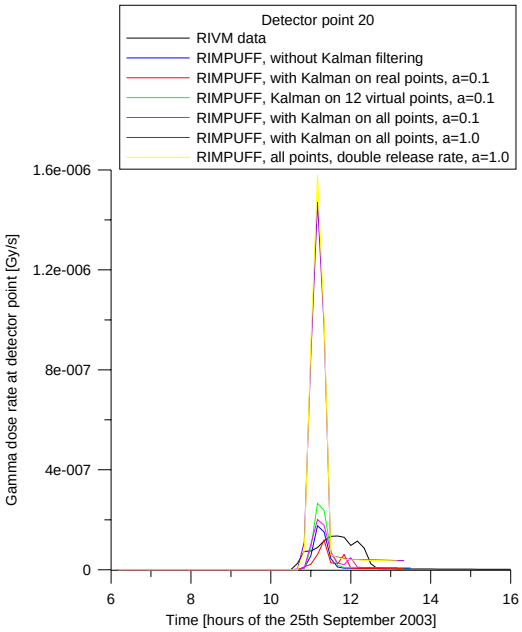
Detector point 20
RIVM data
RIMPUFF, without Kalman filtering
RIMPUFF, with Kalman on real points, a=0.1
RIMPUFF, Kalman on 12 virtual points, a=0.1
RIMPUFF, with Kalman on all points, a=0.1
RIMPUFF, with Kalman on all points, a=1.0
RIMPUFF, all points, double release rate, a=1.0
Gamma dose rate at detector point [Gy/s]
1.6e-006
1.2e-006
8e-007
4e-007
0
6
8
10
12
14
16
Time [hours of the 25th September 2003]

d

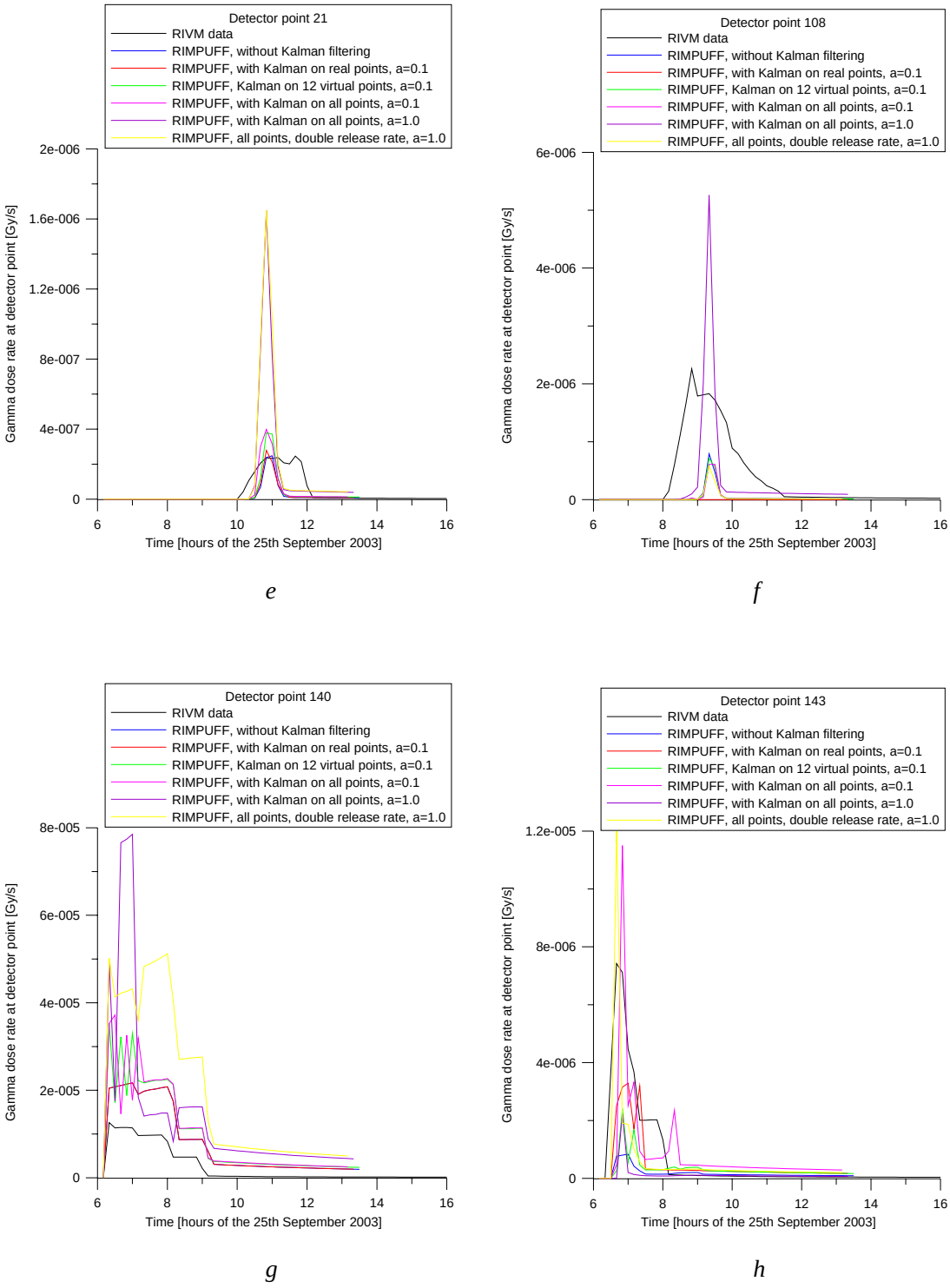

Figure 16: Gamma dose rates at 8 detector points as calculated by RIVM, by RIMPUFF, and by RIMPUFF with Kalman filtering on different extracts of RIVM data. Release as specified. Release rate uncertainty a=0.1.

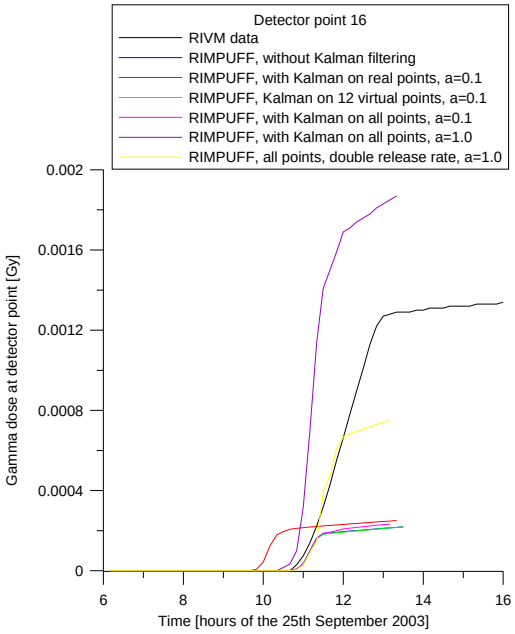
Detector point 16
RIVM data
RIMPUFF, without Kalman filtering
RIMPUFF, with Kalman on real points, a=0.1
RIMPUFF, Kalman on 12 virtual points, a=0.1
RIMPUFF, with Kalman on all points, a=0.1
RIMPUFF, with Kalman on all points, a=1.0
RIMPUFF, all points, double release rate, a=1.0
Gamma dose at detector point [Gy]
0.002
0.0016
0.0012
0.0008
0.0004
0
6
8
10
12
14
16
Time [hours of the 25th September 2003]

a

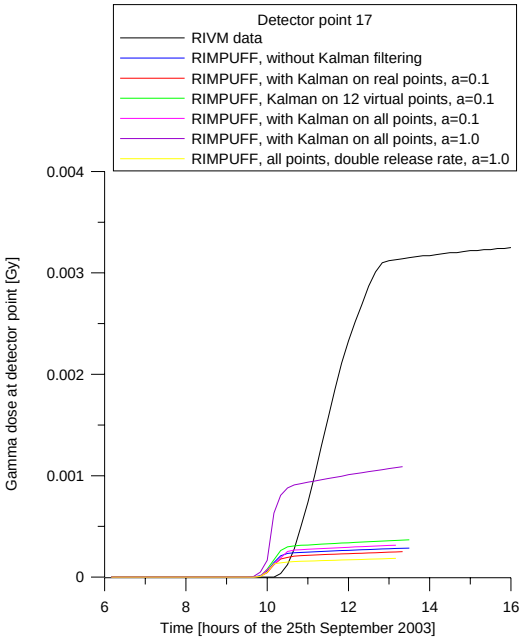
Detector point 17
RIVM data
RIMPUFF, without Kalman filtering
RIMPUFF, with Kalman on real points, a=0.1
RIMPUFF, Kalman on 12 virtual points, a=0.1
RIMPUFF, with Kalman on all points, a=0.1
RIMPUFF, with Kalman on all points, a=1.0
RIMPUFF, all points, double release rate, a=1.0
Gamma dose at detector point [Gy]
0.004
0.003
0.002
0.001
0
6
8
10
12
14
16
Time [hours of the 25th September 2003]

b

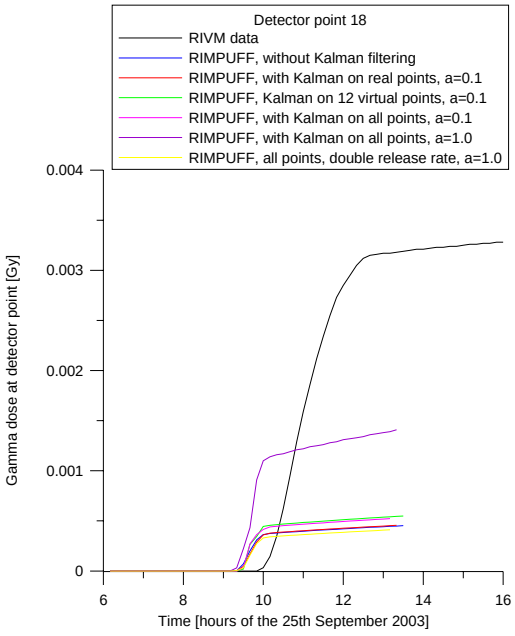
Detector point 18
RIVM data
RIMPUFF, without Kalman filtering
RIMPUFF, with Kalman on real points, a=0.1
RIMPUFF, Kalman on 12 virtual points, a=0.1
RIMPUFF, with Kalman on all points, a=0.1
RIMPUFF, with Kalman on all points, a=1.0
RIMPUFF, all points, double release rate, a=1.0
Gamma dose at detector point [Gy]
0.004
0.003
0.002
0.001
0
6
8
10
12
14
16
Time [hours of the 25th September 2003]

c

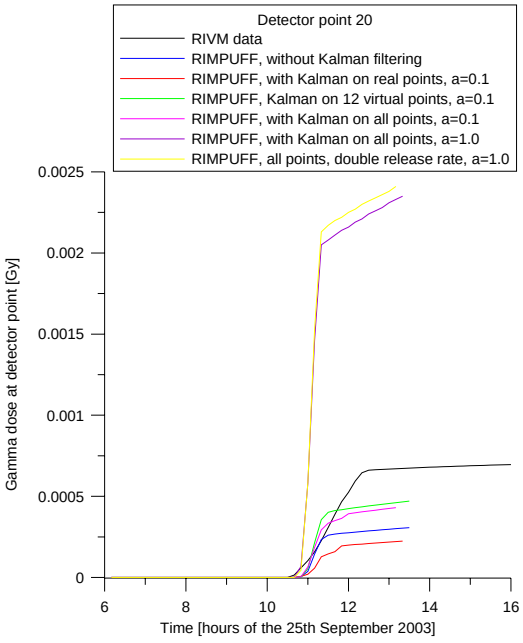
Detector point 20
RIVM data
RIMPUFF, without Kalman filtering
RIMPUFF, with Kalman on real points, a=0.1
RIMPUFF, Kalman on 12 virtual points, a=0.1
RIMPUFF, with Kalman on all points, a=0.1
RIMPUFF, with Kalman on all points, a=1.0
RIMPUFF, all points, double release rate, a=1.0
Gamma dose at detector point [Gy]
0.0025
0.002
0.0015
0.001
0.0005
0
6
8
10
12
14
16
Time [hours of the 25th September 2003]

d

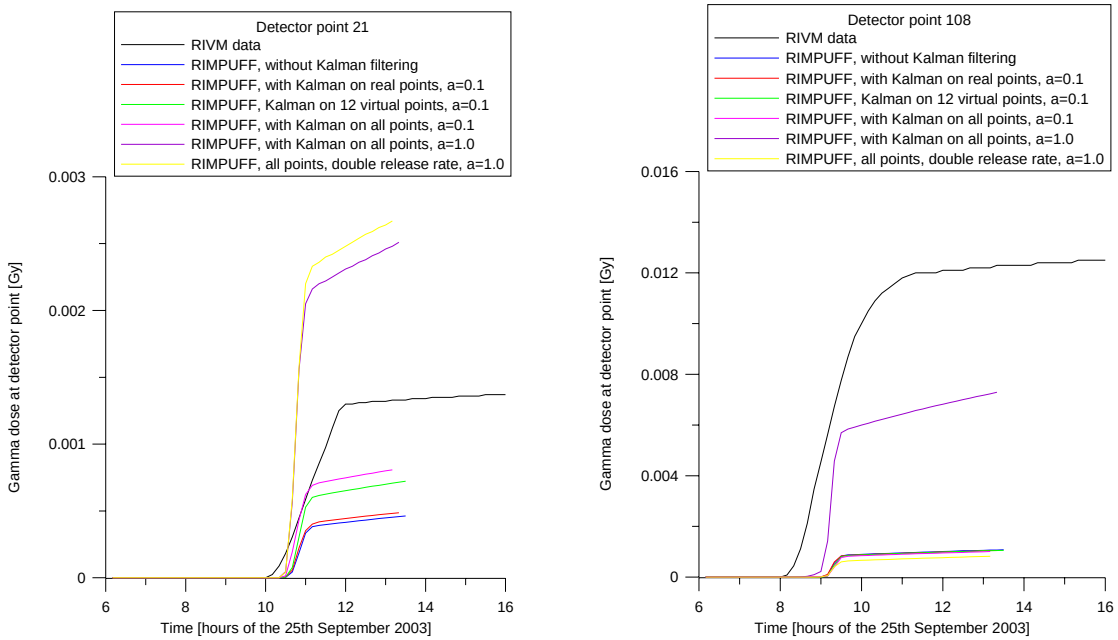

e

f

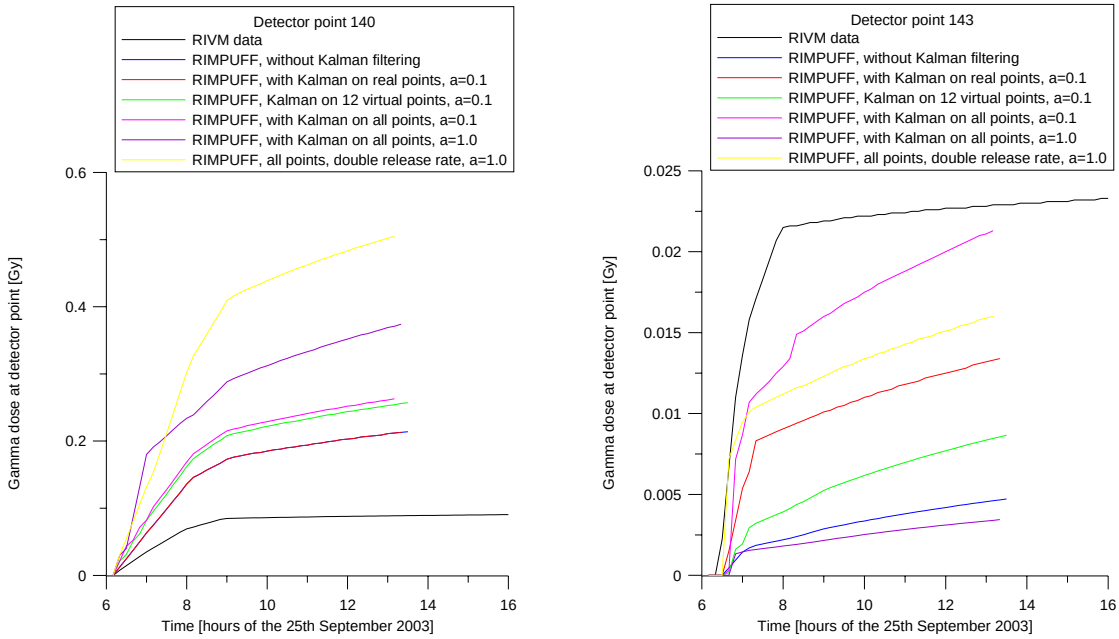

g

h

Figure 17: Gamma doses (time integrated dose rates) at 8 detector points as calculated by RIVM, by RIMPUFF, and by RIMPUFF with Kalman filtering on different extracts of RIVM data. Different releases: as specified, and doubled, and different release uncertainties: a=0.1 and a=1.0.

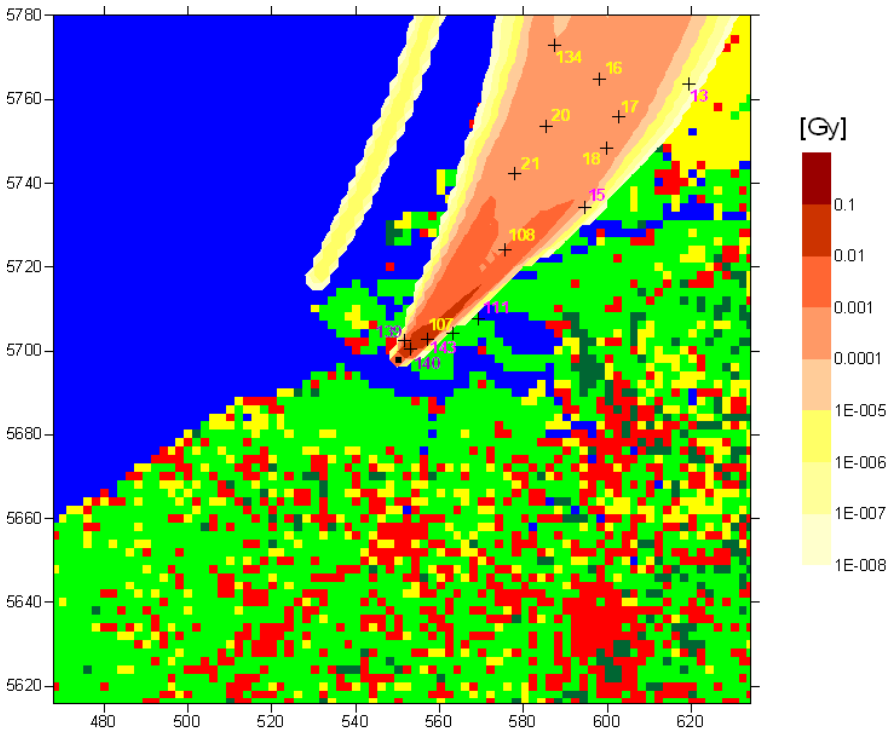

Figure 18: Time integrated dose rates as calculated by RIMPUFF based on one point meteorological data from RIVM (KNMI). Kalman filtering on all detector points, release uncertainty a=0.1.

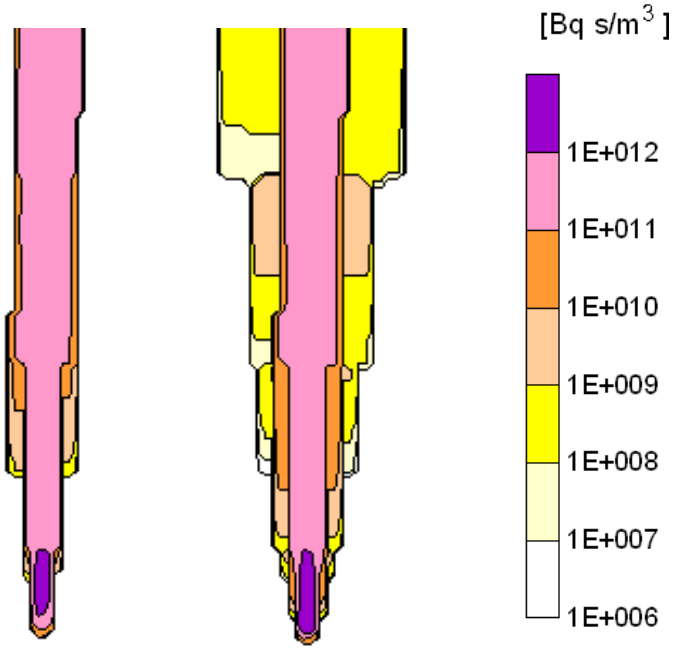

Figure 19: Time integrated air concentration at ground level. Case with 15° uncertainty in the southerly wind direction. a) RIMPUFF, b) mean of 100 ensemble results

9 References

Ehrhardt, J.; Weiss, A. (Eds):
RODOS: Decision Support for Off-Site Nuclear Emergency Management in Europe.
EUR 19144 EN
European Commission
Luxembourg
2000

Gering, F.; Hübner, S.; Faria, A.E.; French, S.:
Model Description of the Deposition Monitoring Module (DEMM).
RODOS(WG5)-TN(99)16
2000

Kalman, R.E.: A new approach to linear filtering and prediction problems.
J. Basic Eng., 82D, 35-45
1960

Kelly, G.N; Ehrhardt, J; Shershakov, V.M.:
Decision support for off-site emergency preparedness in Europe.
Radiation Protection Dosimetry, 64, 1/2, pp129-141
1996

Kovalets, I.; Andronopoulos, S.; Bartzis, J.G.; Gounaris, N.; Kushchan, A.:
Introduction of data assimilation procedures in the meteorological pre-processor of atmospheric dispersion models used in emergency responce systems.
Atmospheric Environment, 38, pp 457-467
2004

Kok, Yvo:
Private communications.
2003

Mikkelsen, T.; Larsen, S.E.; Thykier-Nielsen, S.:
Description of the Risø Puff Diffusion Model.
Nucl. Technol. 67, pp 56-65
1984

Puch, Roberto O.; Astrup, Poul:
An Extended Kalman Filter Methodology for the Plume Phase of a Nuclear Accident.
RODOS(RA5)-TN(01)-07
2002

Rojas-Palma, C.; Gering, F.; Madsen, H.; Puch-Solis, R.; Richter, K.; Müller, H.:
Theoretical framework and practical considerations for data assimilation in off-site nuclear emergency management.
RODOS(RA5)-TN(01)-01
2001

Sass, B.H.:
The DMI Operational HIRLAM Forecasting System, Version 2.3.
DMI Techical Report 94-8
Danish Meteorological Institute
1994

Thykier-Nielsen, S.; Deme, S.; Mikkelsen, T.:
Description of the Atmospheric Dispersion Module RIMPUFF.
RODOS(WG2)-TN(98)-02
1998

10 Appendix A. Kalman filtering

Based on Joseph (1999).

Kalman filtering is a statistically based method to mix model calculations with measurements in order to produce a better estimate of the state of a process than obtainable from either calculations or measurements alone.

The Kalman filter works on a state vector, i.e. a set of state variables central to the process simulated.

10.1 Definitions

η	state vector prediction update uncertainty
x	real state vector
$\overline{x}$	predicted state vector
$\hat{x}$	Kalman filtered state vector
y	measurable real data
$\overline{y}$	predicted data
$\hat{y}$	measured data
$P = E\left[(x-\hat{x})(x-\hat{x})^T\right]$	error covariance matrix
$Q = E\left[\eta\eta^T\right]$	prediction update error covariance
$R = E\left[(y-\hat{y})(y-\hat{y})^T\right]$	measurement error covariance matrix

Here E is the "expected value" operator.

10.2 Conditions

With the following five conditions fulfilled, the Kalman filtering method is optimal in the sense, that it minimizes the error covariances in the P -matrix, i.e. no other method produces smaller error covariances.

1) The evolution in time of the state vector is a linear function of the state vector itself:

   $x^{k+1} = Mx^k + h$ $\quad$ k is the time step index

2) The evolution is prone to white noise.

3) The vector of data to be predicted and measured is a linear function of the state vector:

   $y^k = Hx^k + g$

4) The measurements are prone to white noise.

5) The two noise signals are neither correlated with each other, nor with the state vector, nor with the measurements.

Here M and H are x-independent matrices, and h and g are x-independent vectors.

If these conditions are not all fulfilled, the method may still be useful, but other methods may be constructed, which are more optimal.

Kalman filtering process

$\bar{x} = M\,\hat{x} + h$	prediction update of state vector
$\bar{P} = M\,P\,M^T + Q$	prediction update of error covariance matrix
$\bar{y} = H\,\bar{x} + g$	prediction of the data to be measured
$K = \bar{P}H^T(H\bar{P}H^T + R)^{-1}$	calculation of Kalman gain
$\hat{x} = \bar{x} + K(\hat{y} - \bar{y})$	Kalman filtering
$P = (I - KH)\bar{P}(I - KH)^T + KRK^T$	final update of error covariance matrix

Here I is the unit tensor. For the last equation, an equivalent but, according to Joseph (1999), numerically unstable substitute is often seen in the literature:

$$P = (I - KH)\bar{P}$$

In case the processes are not linear, they may be linearized, and the filter is then called an Extended Kalman filter. M and H are then given as

$$M_{ij} = \frac{\partial x_i^{k+1}}{\partial x_j^k}$$

$$H_{ij} = \frac{\partial \bar{y}_i}{\partial x_j}$$

and all other terms go into *h* and *g*.

10.3 References

Joseph, Peter D:
Kalman Filters.
1999
http://ourworld.compuserve.com/homepages/PDJoseph/kalman.htm

11 Appendix B. Prediction update covariances

11.1 Single puff prediction update covariances

11.1.1 State vector

The state vector part corresponding to a single puff consists of the puffs centre coordinates and its total radioactive inventory:

$\boldsymbol{x} = (x_p, y_p, z_p, q)$

11.1.2 Prediction update linearity

The prediction update of the state vector follows

$$\begin{pmatrix} x \\ y \\ z \\ q \end{pmatrix}_p^{k+1} = \begin{pmatrix} 1 & 0 & 0 & 0 \\ 0 & 1 & 0 & 0 \\ 0 & 0 & 1 & 0 \\ 0 & 0 & 0 & \left(e^{-\lambda \Delta t} - f_{dry+wet}\Delta t\right) \end{pmatrix} \begin{pmatrix} x \\ y \\ z \\ q \end{pmatrix}_p^{k} + \begin{pmatrix} u_x \\ u_y \\ u_z \\ 0 \end{pmatrix} \Delta t$$

As the total deposition fraction $f_{dry+wet}\Delta t$, the decay function $e^{-\lambda \Delta t}$, and the wind velocity vector $\boldsymbol{u} = (u_x, u_y, u_z)$ all can be thought independent of $\boldsymbol{x}$, the prediction update is purely linear in $\boldsymbol{x}$.

11.1.3 Prediction covariances for the coordinates

Looking at the position only, the prediction covariance matrix $\boldsymbol{Q}$ is a function of the uncertainty of the wind vector, of its size and its direction. $\boldsymbol{Q}$ should grow with time for small time steps but level out for increasing time steps. The following is tried:

$$Q = Cov\left[\begin{pmatrix} u_x \\ u_y \\ u_z \end{pmatrix}\begin{pmatrix} u_x \\ u_y \\ u_z \end{pmatrix}^T\right] \min\left(\Delta t, 2T_L\right)^2 = \begin{pmatrix} \overline{u_{x\,c}^2} & \overline{u_x u_{y\,c}} & \overline{u_x u_{z\,c}} \\ \overline{u_x u_{y\,c}} & \overline{u_{y\,c}^2} & \overline{u_y u_{z\,c}} \\ \overline{u_x u_{z\,c}} & \overline{u_y u_{z\,c}} & \overline{u_{z\,c}^2} \end{pmatrix} \min\left(\Delta t, 2T_L\right)^2$$

where subscript c means central moments and T_L is the Lagrangian turbulence time scale. With the wind having speed u, horizontal direction φ (= 270° minus specified incoming direction), and inclination angle ψ, and assuming these parameters uncorrelated and Gaussian distributed around measured 10-minute mean values with standard deviations σ_u, σ_φ, and σ_ψ, the following parameters can be derived:

$$\overline{u_x} = \bar{u}\,\overline{\cos\varphi}$$

$$\overline{u_y} = \bar{u}\,\overline{\sin\varphi}$$

$$\overline{u_z} = 0$$

$$\overline{u_x^2} = \overline{u^2}\,\overline{\cos^2\varphi} = \left(\bar{u}^2 + \sigma_u^2\right)\overline{\cos^2\varphi}$$

$$\overline{u_y^2} = \overline{u^2}\,\overline{\sin^2\varphi} = \left(\bar{u}^2 + \sigma_u^2\right)\overline{\sin^2\varphi}$$

$$\overline{u_z^2} = \overline{u^2}\,\overline{\sin^2\psi} = \left(\bar{u}^2 + \sigma_u^2\right)\overline{\sin^2\psi}$$

$$\overline{u_x u_y} = \overline{u^2}\ \overline{\cos\varphi \sin\varphi} = \left(\overline{u}^2 + \sigma_u^2\right)\ \overline{\cos\varphi \sin\varphi}$$

$$\overline{u_x u_z} = 0$$

$$\overline{u_y u_z} = 0$$

The central moments interesting for the determination of ***Q*** are:

$$\overline{u_{x\,c}^2} = \overline{u_x^2} - \overline{u_x}^2 = \left(\overline{u}^2 + \sigma_u^2\right)\overline{\cos^2\varphi} - \overline{u}^2\,\overline{\cos\varphi}^2$$

$$\overline{u_{y\,c}^2} = \overline{u_y^2} - \overline{u_y}^2 = \left(\overline{u}^2 + \sigma_u^2\right)\overline{\sin^2\varphi} - \overline{u}^2\,\overline{\sin\varphi}^2$$

$$\overline{u_{z\,c}^2} = \overline{u_z^2} - \overline{u_z}^2 = \left(\overline{u}^2 + \sigma_u^2\right)\overline{\sin^2\psi} = \sigma_w^2$$

$$\overline{u_x u_{y\,c}} = \overline{u_x u_y} - \overline{u_x}\,\overline{u_y} = \left(\overline{u}^2 + \sigma_u^2\right)\overline{\cos\varphi \sin\varphi} - \overline{u}^2\,\overline{\cos\varphi}\,\overline{\sin\varphi}$$

$$\overline{u_x u_{z\,c}} = 0$$

$$\overline{u_y u_{z\,c}} = 0$$

With the probability density functions for φ and ψ:

$$p(\varphi) = \frac{1}{\sigma_\varphi\sqrt{2\pi}}\exp\left(-\frac{(\varphi-\varphi_0)^2}{2\sigma_\varphi^2}\right)$$

$$p(\psi) = \frac{1}{\sigma_\psi\sqrt{2\pi}}\exp\left(-\frac{\psi^2}{2\sigma_\psi^2}\right)$$

the trigonometric means become

$$\overline{\cos\varphi} = \cos\varphi_0\ e^{-\sigma_\varphi^2/2}$$

$$\overline{\sin\varphi} = \sin\varphi_0\ e^{-\sigma_\varphi^2/2}$$

$$\overline{\cos^2\varphi} = \frac{1}{2}\left(1 + \cos 2\varphi_0\ e^{-2\sigma_\varphi^2}\right)$$

$$\overline{\sin^2\varphi} = \frac{1}{2}\left(1 - \cos 2\varphi_0\ e^{-2\sigma_\varphi^2}\right)$$

$$\overline{\sin^2\psi} = \frac{1}{2}\left(1 - e^{-2\sigma_\psi^2}\right) = \frac{\sigma_w^2}{\overline{u}^2 + \sigma_u^2}$$

$$\overline{\cos\varphi \sin\varphi} = \cos\varphi_0 \sin\varphi_0\ e^{-2\sigma_\varphi^2}$$

σ_φ and σ_ψ are like σ_u mostly due to the large scale turbulence, for which σ_u, σ_v, and σ_w are calculated for the prediction of puff growth. Derived for $\varphi_0 = 0$, the correspondence between σ_v and σ_φ is given from

$$\sigma_v^2 = \overline{u_y^2} - \overline{u_y}^2 = \overline{u_{y\,c}^2} = \left(\overline{u}^2 + \sigma_u^2\right)\frac{1}{2}\left(1 - e^{-2\sigma_\varphi^2}\right)$$

leading to generally valid

$$e^{-2\sigma_\varphi^2} = 1 - \frac{2\sigma_v^2}{\overline{u}^2 + \sigma_u^2}$$

and equivalently

$$e^{-2\sigma_\psi^2} = 1 - \frac{2\sigma_w^2}{\overline{u}^2 + \sigma_u^2}$$

With $\sigma_u, \sigma_v, \sigma_w$ given by or derived from data of the meteorological preprocessor all the elements of $\boldsymbol{Q}$ are determined.

11.1.4 Prediction covariances for inventory

The inventory update variance is set to

$$Var[qq] = \left[0.05\left(e^{-\lambda\,\Delta t} - f_{dry+wet}\Delta t - 1\right)q\right]^2$$

while all covariances with position coordinates are set to 0.

11.2 Puff to puff update covariances

The puff-to-puff covariance is modelled pretty simple. E.g. for the covariance between the *x* coordinate of puff *n* and the *z* coordinate of puff *m*:

$$Cov[x_n z_m] = F\ 0.5\left(Cov[x_n z_n] + Cov[x_m z_m]\right)$$

where F is a function that goes smoothly from 1 to 0 as the distance between the puff centres go from zero to twice the Lagrangian turbulence length scale. For inventory it is the same formula

$$Cov[q_n q_m] = F\ 0.5\left(Var[q_n q_n] + Var[q_m q_m]\right)$$

while again all inventory-position covariances are set to 0.

Mission

To promote an innovative and environmentally sustainable technological development within the areas of energy, industrial technology and bioproduction through research, innovation and advisory services.

Vision

Risø's research **shall extend the boundaries** for the understanding of nature's processes and interactions right down to the molecular nanoscale.

The results obtained shall **set new trends** for the development of sustainable technologies within the fields of energy, industrial technology and biotechnology.

The efforts made **shall benefit** Danish society and lead to the development of new multi-billion industries.